Molecular Pharmacology Fast Forward. Published on February 15, 2017 as DOI: 10.1124/mol.116.107102
This article has not been copyedited and formatted. The final version may differ from this version.

p38β MAPK signaling mediates exenatide-stimulated microglial β-endorphin expression

Hai-Yun Wu, Xiao-Fang Mao, Hui Fan, and Yong-Xiang Wang

King's Lab, Shanghai Jiao Tong University School of Pharmacy, 800 Dongchuan Road, Shanghai 200240, China (H.Y.W, X.F.M., H.F., Y.X.W.)

Molecular Pharmacology Fast Forward. Published on February 15, 2017 as DOI: 10.1124/mol.116.107102
This article has not been copyedited and formatted. The final version may differ from this version.

Running title: p38β induces microglial β-endorphin expression

Address correspondence to: Yong-Xiang Wang, King's Lab, Shanghai Jiao Tong University School of Pharmacy, 800 Dongchuan Road, Shanghai 200240, China. E-mail: yxwang@sjtu.edu.cn.

Number of text pages: 34

Number of tables: 0

Number of figures: 8

Number of references: 77

Word counts:

Abstract: 246

Introduction: 756

Discussion: 1,563

ABBREVIATIONS: GLP-1R, glucagon-like peptide-1 receptor; cAMP, cyclic adenosine monophosphate; GPCR, G-protein coupled receptor; PKA, protein kinase A; MAPK, mitogen-activated protein kinase; ERK1/2, extracellular signal-regulated kinase1/2; JNK1/2, C-Jun N-terminal kinase1/2; CREB, cAMP response element binding protein; POMC, proopiomelanocortin; TNF-α, tumor necrosis factor-α; IL, interleukin; siRNA, short-interfering RNA; LPS, lipopolysaccharides; DDA, 2',5'-dideoxyadenosine; DOTAP, 1,2-dioleoyl-3-trimethylammonium-propane; DAPI, 4',6-diamidino-2-phenylindole; ANOVA, analysis of variance; EC_{50}, half-effective concentration; SNK test, SNK test.

Molecular Pharmacology Fast Forward. Published on February 15, 2017 as DOI: 10.1124/mol.116.107102
This article has not been copyedited and formatted. The final version may differ from this version.

Abstract

Upon recent discovery, it has been established that activation of glucagon-like peptide-1 receptors (GLP-1Rs) exhibits neuroprotection and antinociception through microglial β-endorphin expression. This study aims to explore its underlying signaling mechanisms. GLP-1Rs and β-endorphin were co-expressed in primary cultures of microglia. Treatment with the GLP-1R agonist exenatide concentration-dependently stimulated microglial expression of the β-endorphin precursor gene POMC and peptide, with EC_{50} values of 4.1 and 7.5 nM, respectively. Exenatide also significantly increased intracellular cAMP levels and expression of *p*-PKA, *p*-p38 and *p*-CREB in cultured primary microglia. Furthermore, exenatide-induced microglial expression of POMC was completely blocked by reagents that specifically inhibit adenylyl cyclase and activation of PKA, p38 and CREB. In addition, exenatide-induced microglial p38 phosphorylation and POMC expression were eliminated by knockdown of p38β (but not p38α) using siRNA. In contrast, LPS-increased microglial activation of p38 and expression of proinflammatory factors (including TNF-α, IL-1β and IL-6) were partially suppressed by knockdown of p38α (but not p38β). Exenatide-induced phosphorylation of p38 and CREB was also totally blocked by the PKA inhibitor and siRNA/p38β, but not by siRNA/p38α. The 7-day intrathecal injections of siRNA/p38β (but not siRNA/p38α) completely blocked exenatide-induced spinal p38 activation, β-endorphin expression and mechanical antiallodynia in rats of established neuropathy, although siRNA/p38β and siRNA/p38α were not antiallodynia. Our results, for the first time, have drawn a causal relationship between the PKA-dependent p38β MAPK/CREB signal cascade and GLP-1R agonism-mediated microglial β-endorphin expression. Differential role of p38α and p38β activation in inflammation and nociception was also highlighted.

Molecular Pharmacology Fast Forward. Published on February 15, 2017 as DOI: 10.1124/mol.116.107102
This article has not been copyedited and formatted. The final version may differ from this version.

Introduction

Glucagon-like peptide-1 receptors (GLP-1Rs) in pancreatic islet β-cells have been implicated in the treatment of type 2 diabetes mellitus (Graaf et al., 2016; Koole et al., 2013). Activation of GLP-1Rs in the central nervous system also exhibits neuroprotection in preclinical animal models of neurodegenerative disorders, including Parkinson's disease, Alzheimer's disease, amyotrophic lateral sclerosis, multiple sclerosis, peripheral neuropathy, and ischemia and stroke (Hansen et al., 2015; Harkavyi and Whitton, 2010; Holscher, 2012; Jia et al., 2015; Kim et al., 2009). Our laboratory also recently revealed that agonism of spinal GLP-1Rs by peptidic, non-peptidic and herbal iridoid agonists produced antinociception in a variety of rodent pain models of neuropathy, inflammation, bone cancers, and diabetes (Fan et al., 2015; Gong et al., 2014b; Zhu et al., 2014; Xu et al., 2017). GLP-1R in pancreatic islet β-cells during episodes of hyperglycemia evokes insulin synthesis (Baggio and Drucker, 2007; Lee and Jun, 2014). In contrast, activation of GLP-1Rs in the hippocampus and spinal dorsal horn leads to microglial expression of β-endorphin (Gong et al., 2014b; Jia et al., 2015). However, the signal mechanisms underlying GLP-1R-mediated microglial β-endorphin expression remains to be determined.

The GLP-1R belongs to the class B of the G-protein coupled receptor (GPCR) family, with signaling via multiple G-proteins, including $G_{\alpha s}$, $G_{\alpha i}$, $G_{\alpha o}$, and $G_{\alpha q/11}$ (Hallbrink et al., 2001). Multiple signal transduction pathways have been characterized for GLP-1R-induced insulin synthesis (Baggio and Drucker, 2007), among which the cAMP (cyclic adenosine monophosphate)/PKA (protein kinase A) signaling through $G_{\alpha s}$ was identified to be a classical pathway for insulin secretion (Drucker et al., 1987; Koole et al., 2013). Moreover, the cAMP response element binding protein (CREB) signaling was shown to be a crucial transcription factor for expression of insulin and the β-endorphin precursor proopiomelanocortin (POMC) in pancreatic and pituitary cells (Dalle et al., 2011; Kraus and Hollt, 1995). These findings prompted us to illustrate the causal association between the cAMP/PKA/CREB signaling pathway and exenatide-induced β-endorphin expression

in microglia.

Mitogen-activated protein kinases (MAPKs), including p38, c-Jun N-terminal kinase1/2 (JNK1/2), and extracellular signal regulated kinase1/2 (ERK1/2) isoforms (Johnson and Lapadat, 2002), play critical roles in microglial activation (Milligan and Watkins, 2009). However, GLP-1R-induced p38 activation in insulinoma cells promoted insulin secretion (Kemp and Habener, 2001), whereas it inhibited rapamycin-induced p38 activation in pancreatic β-cells (Kawasaki et al., 2010). ERK1/2 in β-cells and adipose tissue macrophages was markedly activated (MacDonald et al., 2002; Montrose-Rafizadeh et al., 1999) or inactivated (Lee et al., 2012). GLP-1R activation in pancreatic β cells and macrophages was anti-inflammatory and anti-apoptotic by inhibiting JNK1/2 activation (Kawasaki et al., 2010; Lee et al., 2012). Previous data on p38 involvement in the antinociceptive effect of the GLP-1R iridoid agonist shanzhiside methylester (Fan et al., 2016) led us to explore the roles of MAPK activation in exenatide-mediated β-endorphin expression in microglia.

The p38 MAPK family consists of 4 members, *i.e.*, p38α, p38β, p38δ and p38γ. Among these four isoforms, only p38α and p38β are mainly expressed in microglia in the central nervous system (Dong et al., 2014). Although p38α and p38β share approximately 80% homology of their protein sequences, they exhibit differential biological functions (Li et al., 2008). Knockout/mutation of p38α (but not p38β) attenuated microglial expression of proinflammatory cytokines, tumor necrosis factor-α (TNF-α), interleukin (IL)-6 and IL-1β (Bachstetter et al., 2011; Xing et al., 2011), and activated microglia-induced neuron degeneration (Xing et al., 2013). In contrast, p38β was recently identified to play a critical role in the survival of endothelial cells, myocytes and fibroblasts (Si and Liu, 2009; Wang et al., 1998). Accordingly, identification of the roles of p38α and p38β in exenatide-induced β-endorphin expression is an area worth exploration.

This study mainly aimed to characterize the signal transduction mechanisms in cultured primary microglia by which exenatide stimulates microglial expression of β-endorphin, with focus on the involvement of the subtypes of MAPKs and isoforms

of p38 MAPK, as well as their upstream and downstream signals. In parallel to β-endorphin expression, we assessed exenatide on intracellular cAMP levels and phosphorylation of PKA, MAPKs and CREB. In order to reveal the causal association, selective inhibitors of each signaling molecule were employed to intervene β-endorphin expression. Since selective inhibitors of p38β and p38α activation are not available (Coulthard et al., 2009; O'Keefe et al., 2007), RNA interference technology was employed to measure p38α and p38β phosphorylation and intervention of exenatide-induced β-endorphin expression and antinociception in neuropathy. Our results, for the first time, demonstrated that the cAMP/PKA/p38β/CREB signal transduction pathway entirely mediates exenatide-induced β-endorphin expression and highlight differential roles of p38α and p38β in inflammation and nociception.

Materials and Methods

Drugs. Exenatide was obtained from Kaijie Bio-Pharmaceuticals (Chendu, China) and the specific adenylate cyclase inhibitor DDA (2',5'-dideoxyadenosine), PKA inhibitor H-89, JNK1/2 inhibitor SP600125, ERK1/2 inhibitor U0126, CREB inhibitor KG501, and p38 inhibitor SB203580 were purchased from Selleck Chemicals (Houston, TX). We followed references and chose the above specific inhibitors at certain concentrations/doses (see below), although their specificity on microglial cells may not be validated.

Laboratory rodents. Male 1-day-old neonatal and adult (8-10-week-old) Wistar rats were obtained from the Experimental Animal Institute (Shanghai, China). On a 12-hour light/dark cycle, the adult rats were placed in a humidity- and temperature-controlled environment with water and food *ad libitum*. The adult rats were accustomed to the environment for 3-5 days before surgery and were randomly assigned to research groups. The animal procedures were approved by the Shanghai Jiao Tong University Experimental Animal Care and Welfare Committee and followed the regulatory animal care guidelines of the National Institutes of Health.

Primary Cultures of Microglia. As the cortex harvested more cells, its

microglial cells were collected for this study. Briefly, the cortex was harvested from neonatal rats and its meanings were removed, and the isolated cortex tissues were then minced and incubated in 0.05% trypsin. The dissociated cells were suspended in DMEM supplemented with 10% fetal bovine serum (Gibco, New York), penicillin (100 U/mL) and streptomycin (100 μg/mL). The suspension cells, plated in 75 cm^2 tissue cultural flasks (1×10^7 cells/flask) precoated with poly-L-lysine (0.1 mg/mL), were incubated in a humidified atmosphere with 5% CO_2 at 37°C, with replenishment each 3 days. Being cultured for 8 days, the confluent mixed glial cultures were collected as floating suspensions by shaking (260 rpm) at 37°C for 2 hours. The unattached cells were removed by the serum-free DMEM after the aliquots were placed to plates (Gong et al., 2014b). Harvested microglial cells showed a characterized morphology of small cell body endowed with thin processes, with a purity of more than 95% measured by the IBA-1 immunostaining.

Isolation and Reverse Transcription of RNA and Real-Time Quantitative PCR Measurement. Total RNAs of primary microglia and spinal homogenates were isolated and purified on ice by using the TRIzol reagent (Invitrogen, Grand Island, NY). Reverse transcription was performed using a qPCR RT kit (Toyobo, Osaka, Japan) and Real-time quantitative PCR measurement was performed using the RealmasterMix (SYBR Green I) (Toyobo). The used primers followed the sequences: 5′-CTCCCTGGCACCCATGAAAT-3′ (p38β forward) and 5′-GACACATCCGTGCATTCGTG-3′ (p38β reverse) (NM001109532.2), 5′-AGCTGCGTCGAACCGTG-3′ (p38α forward) and 5′-GGGT CACCAGGTACACATCG-3′ (p38α reverse) (NM031020.2), 5′-CCCTCCTGCTTC AGACCTCCA-3′ (*POMC* exon 2-3 forward) and 5′-TCTCTTCCTCCGCACGC CTCT-3′ (*POMC* exon2-3 reverse) (Sitte et al., 2007), 5′-CCAAGGTCATCCATG ACGAC-3′ (*gapdh* forward) and 5′-TCCACAGTCTTCTGAGTGGC-3′ (*gapdh* reverse) (Gong et al., 2014b), 5′-CCCCGACTATGTGCTCCTCAC-3′ (TNF-α forward) and 5′-AGGGCTCTTGATGGCGGA-3′ (TNF-α reverse); 5′-GGAAGG CAGTGTCACTCATTGTG-3′ (IL-1β forward) and 5′-GGTCCTCATCCTGGAA GCTCC-3′ (IL-1β reverse), and 5′-GGGACTGATGTTGTTGACAGCC-3′ (IL-6

forward) and 5′-CATATGTAATTAAGCCTCCGACTTGTG-3′ (IL-6 reverse) (Raghavendra et al., 2004). All the primers were validated to be specific by melting curves. Relative expression was calculated with $2^{-\Delta\Delta CT}$ method after normalizing targeting gene Ct values with *gapdh* Ct values (Gong et al., 2014b).

Western Blotting. Homogenized spinal lumbar enlargements (L4-L6) and cultured microglia were lysed in the immunoprecipitation analysis buffer containing the protease inhibitor phenylmethylsulfonyl fluoride and phosphatase inhibitor cocktail A/B. Protein supernatants were obtained and their concentrations were measured by using a bicinchoninic acid assay (Beyotime Institute of Biotechnology, Jiangsu, China) (Holz et al., 1999; Holz et al., 1995). Proteins were separated by SDS-PAGE (10%) and further transferred to polyvinylidene fluoride membranes using an electrophoretic method. The membrane was blocked by skim milk (5%) in TBS containing Tween 20 (0.1%) and further incubated with the primary antibody against *p*-PKA (1:500, Santa Cruz Biotech, Santa Cruz, CA), *p*-p38 (1:1,000, Cell Signaling Technology, Danvers, MA), *p*-JNK1/2 (1:1,000, Cell Signaling Technology), *p*-ERK1/2 (1:1,000, Cell Signaling Technology), *p*-CREB (1:1,000, Cell Signaling Technology), p38β (1:500, Protein Tech Group, Chicago, IL), p38α (1:1,000, Cell Signaling Technology), and GAPDH (1:5,000, Protein Tech Group) overnight at 4°C by slight shaking. The protein bands were visualized under an Odyssey Infrared Imaging system (Li-Cor Biosciences, Lincoln, NE) after one hour incubation at 37°C with the Dylight 680 conjugated anti-mouse IgG (1:10,000, Rockland Immunochemicals, Gilbertsville, PA) and Dylight 800 conjugated anti-rabbit IgG (1:10,000, Rockland Immunochemicals). The intensity of the protein band was measured using the Image J software, and the relative protein expression level was calculated after normalization to the GAPDH protein. Protein samples from 3 to 4 batches of cultured cells were used for western blotting (Fan et al., 2016; Gong et al., 2014b).

Immunofluorescence Staining. Cultured primary microglia were seeded on poly-L-lysine-coated coverslips that had been placed at the bottom of the 12-well plates (5×10^4 cells/well). After overnight culture, cells were fixed in 4% PFA for 1

hour and further incubated in PBS containing 10% goat serum and 0.5% X-100 for 1 hour. The cell flasks were then incubated with the rat GLP-1R antibody (1:200, Abcam, Cambridge, UK), β-endorphin antibody (1:200, Abcam) and IBA-1 antibody (1:200, Merck Millipore, Temecula, CA) at 4°C overnight, followed by incubation with the Alexa-555-conjugated goat anti-rabbit secondary antibody (1:200, Life Technologies, Carlsbad, CA,) and Alexa-488-conjugated goat anti-mouse secondary antibody (1:200, Life Technologies) for 1 hour at 37°C. Expression of GLP-1R, β-endorphin and IBA-1 was visualized under a laser scanning confocal microscope (Leica Microsystems). The nucleic staining reagent 4',6-diamidino-2-phenylindole (DAPI, 1 μg/mL, Sigma-Aldrich) was used to stain cell nuclei. Colocalization was identified using the Image J software equipped with a colocalization finder, under which colocalized pixels appeared white (Gong et al., 2014b).

cAMP Accumulation Assay. After 30-min incubation, exenatide-stimulated intracellular cAMP levels in cell lysates containing 3-isobutyl-1-methylxanthine, a specific inhibitor of the cyclic nucleotide phosphodiesterase, were measured using a commercial enzyme immunoassay kit (R&D Systems. Minneapolis, MN) (Koole et al., 2010). The total intracellular protein concentrations were determined using the standard bicinchoninic acid assay (Beyotime Institute of Biotechnology).

β-Endorphin Assay. Exenatide-induced β-endorphin expression in cultured primary microglia was determined using an enzyme-linked fluorescent immunoassay kit (Phoenix Pharmaceuticals, Burlingame, CA). Based on the manufacturer's introduction, it had no cross-reactivity with leu-enkephalin (0%) or met-enkephalin (0%), but it showed 60% and 100% cross-reactivity with γ-endorphin and α-endorphin, respectively. Cultured primary microglia were placed in 24-well plates (1×10^5 cells/well) and washed with warm DMEM (1 mL) in the presence of *N*-(2-hydroxyethyl) piperazine-N'-2-ethanesulfonic acid (15 mmol/L) and BSA (2 mg/mL). The β-endorphin titers in supernatants were determined using the fluorescent assay after microglial cells were stimulated with exenatide for 2 hours (Chen et al., 2012b; Gong et al., 2014b).

RNA Interference. The short-interfering RNA (siRNA) targeting p38α/MAPK14

and p38β/MAPK11, and the nonspecific oligonucleotides (oligos) were designed and synthesized by GenePharma (Shanghai, China) in the following sequences: p38α/MAPK14, 5′-GCACGAGAAUGUGAUUGGUTT-3′/5′-ACCAAUCACAUUCUCGUGCTT-3′; p38β/MAPK11, 5′-GCACGAGAACGUCAUAGGATT-3′/5′-UCCUAUGACGUUCUCGUGCTT-3′, and the nonspecific oligos, 5′-UUCUCCGAACGUGUCACGUTT-3′/5′-ACGUGACACGUUCGGAGAATT-3′. To formulate siRNA, the lipofectin DOTAP (1,2-dioleoyl-3-trimethylammonium-propane, Avanti Polar Lipids, Alabaster, AL) was added according to the manufacturer's instructions. For microglial transfection, the cells were seeded into 24-well/6-well plates and the siRNA-DOTAP complex was added with supplement of basic DMEM medium (final siRNA concentration of 5 μg/mL) and incubated for 5 hours. cells were further cultured for 24 hours routinely after transfection. For the spinal transfection, the siRNA-DOTAP complex was intrathecally injected successively for 7 days.

Rat Intrathecal Catheterization and Injection. A PE-10 catheter (Clay Adams, Parsippany, NJ) was intrathecally inserted into the spinal lumbar in the rat under isoflurane anesthesia run by a Ugo Basile Gas Anesthesia System (Comerio, Italy). The correct placement of the catheter was confirmed by intrathecal administration of lidocaine 2 days following recovery from anesthesia. Rats that had no motor impairments after catheterization and developed immediate paralysis of bilateral hindlimbs after lidocaine were selected for the study. For intrathecal administration, a 10-μL of the drug solution was administered followed by a 15-μL normal saline flush (Wei et al., 2016).

Rat Model of Neuropathy and Mechanical Threshold Assessment. Rats were anesthetized under inhaled isoflurane anesthesia. The left spinal nerves (L5 and L6) were isolated and tightly ligated with 6-0 silk sutures. The lumbar fascia and skin were closed by 4-0 resorbable polyglactin sutures after ligation and the rats were allowed to recover (Kim and Chung, 1992). Since intrathecal delivery was needed in neuropathic rats in the present study, the intrathecal catheterization was performed at the same time just before spinal nerve injury. After surgery, rats that had significant

mechanical allodynia in the ipsilateral hindpaws with withdrawal thresholds <8 g and had no major motor impairments were chosen for the investigation. Drug testing started one week after spinal nerve ligation.

For assessment of mechanical allodynia, an examiner who was blind to the treatment groups tested mechanical thresholds in both hindpaws using a 2290 CE electrical von Frey hair (IITC Life Science, Woodland Hills, CA) which could generate a force ranged from 0.1 to 90 g. The evoked withdrawal thresholds were determined by stimulation of the hindpaw when the rat stood on a metal grid. Increasing force was applied to stimulate the footpad until a sudden withdrawal response and the lowest force was the threshold, which was averaged from triplicate measurements within approximately 30 seconds (Zhang et al., 2013).

Statistical Analysis. To determine the half-effective concentration (EC_{50}) of the concentration-response curve, values of response (Y) were fitted by non-linear least-squares curves to the relation $Y=a+bx$ where $x=[C]^n/(EC_{50}{}^n+[C]^n)$, yielding a minimum residual sum of squares of deviations from the theoretical curve. The EC_{50} and b (maximum effect) values were projected (Wang and Pang, 1993).

Data are shown as means ± standard deviation (SD). The unpaired and two-tailed Student t-test and one-way analysis of variance (ANOVA) were used to evaluate statistical significance. The post-hoc Student-Newman-Keuls (SNK) test was performed when a statistical significance was achieved for the drug (concentration or dose) in the ANOVA analysis. The Version 7.00 of the GraphPad Prism software (GraphPad Software, La Jolla, CA) was used for the concentration-response analysis and statistical evaluation. $P < 0.05$ was considered to be statistically significant.

Results

Exenatide Stimulated β-Endorphin Overexpression in Primary Microglia. The peptidic, nonpeptidic and small molecule agonists of the GLP-1Rs stimulated β-endorphin expression and release in microglia originating from the cortex (Fan et al., 2015; Fan et al., 2016), hippocampus (Jia et al., 2015) and spinal cord (Gong et al.,

2014b). To confirm co-expression of GLP-1R and β-endorphin, we performed the double immunofluorescence staining of respective GLP-1R and the microglial marker IBA-1, β-endorphin and IBA-1, and β-endorphin and GLP-1R in cultured primary microglia originating from the cortex. GLP-1Rs (Fig. 1A-D) and β-endorphin (Fig. 1E-H) were found to be colocalized in microglial cells (labeled by IBA-1), and β-endorphin was also colocalized with GLP-1Rs in microglia (Fig. 1I-L).

We further constructed a concentration-response curve of the GLP-1R peptidic agonist exenatide (0.3, 1, 3, 10, 30 and 100 nM) on β-endorphin expression and release in cultured primary microglia. The POMC gene expression in microglia and β-endorphin levels in the cell cultural medium were measured 2 hours later using respective real-time quantitative PCR and a fluorescent immunoassay assay kit. Its time point selected was based on the higher measurement sensitivity after POMC and β-endorphin accumulation. Incubation with exenatide concentration-dependently increased POMC expression, with an EC_{50} of 4.1 nM (Fig. 1M). In agreement with the POMC expression, the β-endorphin level in the cell cultural medium was concentration-dependently elevated, with an EC_{50} of 7.4 nM (Fig. 1N). We thus selected the sub maximal concentration of 10 nM for the later studies of signal mechanisms. As exenatide stimulated POMC expression and β-endorphin release in parallel, the POMC expression was only measured for the following studies.

The cAMP/PKA Signaling Mediated Exenatide-Stimulated POMC Overexpression. Incubation of exenatide (10 and 100 nM) with cultured primary microglia for 30 minutes maximally elevated the intracellular cAMP level measured by using a commercial fluorescent immunoassay kit ($P < 0.05$, one-way ANOVA followed by post-hoc SNK tests) (Fig. 2A). Exenatide-stimulated PKA activation was later determined using western blotting. Treatment with exenatide (10 nM) for 30 minutes significantly increased PKA phosphorylation by 80% ($P < 0.05$, unpaired and two-tailed Student t-test) (Fig. 2B). To further determine whether activation of the cAMP/PKA signaling was causally associated with exenatide-stimulated POMC expression, pharmacological inhibition of adenylate cyclase and PKA phosphorylation was tested. Although treatment with the specific adenylate cyclase inhibitor DDA

(100 μM) and PKA inhibitor H-89 (10 μM) (Chijiwa et al., 1990; Engh et al., 1996; Liu et al., 2014; Liu et al., 2012; Mitsuya et al., 1987) did not affect basal POMC expression, their pretreatment (1 hour earlier) completely attenuated exenatide-increased expression of POMC ($P < 0.05$, one-way ANOVA) (Fig. 2C, D).

p38 Phosphorylation Mediated Exenatide-Stimulated POMC Overexpression. To explore whether the MAPK signaling played a causal role in exenatide-induced β-endorphin overexpression measured by using western blotting, phosphorylation of p38, JNK1/2, and ERK1/2 was analyzed. Treatment with 10 nM of exenatide for 15, 30, or 60 minutes could time-dependently stimulate p38 phosphorylation with a peak effect at 30 minutes ($P < 0.05$, one-way ANOVA) (Fig. 3A). However, it did not significantly alter phosphorylation of either ERK1/2 or JNK1/2 during the observation period up to 60 minutes (Fig. 3B, C). The time point of 30 minutes was then selected for the later phosphorylation measurements.

To further explore whether p38 activation was causally associated with exenatide-mediated POMC overexpression, pharmacological inhibition on activation of p38, JNK1/2 and ERK1/2 was tested. Incubation with the selective p38 inhibitor SB203580 (50 μM) (Lali et al., 2000; Pyo et al., 1999; Yang et al., 2007), ERK1/2 inhibitor U0126 (50 μM) (DeSilva et al., 1998) and JNK1/2 inhibitor SP600125 (50 μM) (Bennett et al., 2001) did not alter basal POMC expression (Fig. 3D-F). However, pretreatment (1 hour earlier) with SB203580 completely blocked exenatide-stimulated overexpression of POMC ($P < 0.05$, one-way ANOVA) (Fig. 3D). In contrast, neither U0126 nor SP600125 significantly suppressed exenatide-increased POMC expression (Fig. 3E, F).

To confirm the PKA dependency of exenatide-stimulated p38 activation in cultured primary microglia, incubation with exenatide (10 nM) for 30 minute significantly stimulated p38 phosphorylation, which was completely blocked by pretreatment (1 hour prior to) with 10 μM of H-89 ($P < 0.05$, one-way ANOVA) (Fig. 3G).

p38β Phosphorylation Mediated Exenatide-Stimulated POMC Overexpression. As shown in Fig. 4A, transfection with siRNA/p38α for 5 hours did

not significantly alter p38β mRNA expression compared to the nonspecific oligo control, but markedly reduced expression of p38α mRNA by 57% ($P < 0.05$, one-way ANOVA). Similarly, siRNA/p38α reduced the levels of p38α (but not p38β) protein by 58% ($P < 0.05$, one-way ANOVA) (Fig. 4B). Moreover, compared to the nonspecific oligo control, transfection with siRNA/p38β significantly reduced expression of p38β (but not p38α) mRNA and protein by 57% and 53%, respectively ($P < 0.05$, one-way ANOVA) (Fig. 4C, D).

Our additional study was tried to reveal the specific effects of p38α and p38β silencing on exenatide-stimulated p38 activation and POMC expression. Transfection with siRNA/p38β completely blocked exenatide-stimulated total p38 phosphorylation, compared to the nonspecific oligo control ($P < 0.05$, one-way ANOVA) (Fig. 4E). On the contrary, siRNA/p38α failed to alter exenatide-induced total p38 phosphorylation. In addition, transfection with siRNA/p38β but not siRNA/p38α completely attenuated exenatide-stimulated overexpression of POMC ($P < 0.05$, one-way ANOVA) (Fig. 4F).

p38α Phosphorylation Mediated LPS-Stimulated Overexpression of Proinflammatory Cytokines. In comparison, the possible attenuation of siRNA/p38α and siRNA/p38β on microglial expression of proinflammatory cytokines was also tested. Treatment with LPS (lipopolysaccharides, *Escherichia coli* strain O26:B6, Sigma-Aldrich) for 1 hour significantly increased microglial totalp38 phosphorylation, which was 43% reduced by pretransfection with siRNA/p38α ($P < 0.05$, one-way ANOVA). On the contrary, knockdown of p38β gene failed to affect LPS-stimulated p38 phosphorylation (Fig. 5A). Furthermore, treatment with LPS in microglia dramatically increased expression of TNF-α, IL-1β and IL-6 by 20-, 36- and 880-fold, respectively. Pretransfection with siRNA/p38α partially attenuated LPS-induced overexpression of TNF-α, IL-1β and IL-6 by 40%, 33% and 24%, respectively ($P < 0.05$, one-way ANOVA). However, siRNA/p38β was not able to significantly reduce LPS-induced overexpression of proinflammatory cytokines (Fig. 5B-D).

p38β Phosphorylation Mediated Exenatide-Induced Spinal POMC Overexpression and Mechanical Antiallodynia. To further confirm the causal role

of p38β isoforms in exenatide-mediated spinal POMC overexpression and mechanical antiallodynia, specific siRNA/p38α and siRNA/p38β were employed in rats of neuropathy established 1 week earlier. Five groups of rats of neuropathy received consecutive 7-day intrathecal injections of the vehicle, nonspecific oligos (5 μg/day), siRNA/p38α (5 μg/day) or siRNA/p38β (5 μg/day). Mechanical withdrawal thresholds were measured once daily in both hindpaws prior to each siRNA injection. Multi-daily intrathecal injections of either siRNA/p38α or siRNA/p38β was not able to alter basal withdrawal thresholds in both hindpaws (Fig. 6A). On the eighth day, the rats received a single bolus intrathecal injection of normal saline (10 μL) or exenatide (100 ng) and their hindpaws were subjected to mechanical stimuli 1 hour post-injection. Intrathecal exenatide in ipsilateral hindpaws produced marked mechanical antiallodynia, which was totally suppressed by knockdown of p38β gene ($P < 0.05$, one-way ANOVA). On the contrary, the 7-day intrathecal injections of siRNA/p38α failed to significantly suppress exenatide-induced mechanical antiallodynia (Fig. 6B).

Upon finishing of behavioral assessment, the spinal cord enlargements were isolated and divided into two parts for measurement of expressions of p38α and p38β (mRNA and protein) and POMC mRNA. The remaining portion was further divided into the contralateral and ipsilateral side for p38 phosphorylation measurement. Compared to the nonspecific oligo control, the consecutive 7-day intrathecal injections of siRNA/p38α effectively reduced expression of p38α mRNA and protein by 68% and 54%, respectively ($P < 0.05$, one-way ANOVA), without significant reduction of p38β mRNA and protein expression (Fig. 6C, D). On the other hand, siRNA/p38β compared to the nonspecific oligo control reduced p38β gene and protein expression by 40% and 47%, respectively ($P < 0.05$, one-way ANOVA), without reducing expression of p38α gene and protein (Fig. 6E, F).

Further analyses were undertaken to test the possible blockade effects of the p38 isoform gene silencing on exenatide-stimulated spinal p38 phosphorylation in the spinal cords of rats that had been subjected to spinal nerve ligation two weeks earlier. As shown in the representative gels, the expression of p38 total phosphorylation in the

contralateral spinal cord was not apparently different from that in the ipsilateral spinal cord. However, intrathecal exenatide significantly elevated total p38 phosphorylation in both contralateral and ipsilateral spinal cord by the same degree. The stimulatory effect of exenatide was completely suppressed by intrathecal injection of siRNA/p38β ($P < 0.05$, one-way ANOVA) (Fig. 6G). On the contrary, intrathecal siRNA/p38α failed to significantly reduce exenatide-increased spinal total p38 activation. Fig. 6H showed the summarized group results from scanned gels.

Moreover, we tested to uncover which p38 isoform was responsible for exenatide-stimulated spinal POMC overexpression. In agreement with cultured primary microglia, intrathecal exenatide increased spinal expression of POMC mRNA, which was entirely inhibited by knockdown of spinal p38β gene, compared to the nonspecific oligo control ($P < 0.05$, one-way ANOVA). On the contrary, intrathecal siRNA/p38α was unable to significantly attenuate exenatide-stimulated spinal POMC overexpression (Fig. 6I).

CREB Phosphorylation Mediated Exenatide-Stimulated POMC Overexpression. We further tested whether exenatide-induced microglial POMC overexpression was via CREB phosphorylation. Treatment with exenatide (10 nM) in cultured primary microglia for 30 minutes significantly elevated CREB phosphorylation by 113% ($P < 0.05$, unpaired and two-tailed Student t-test) (Fig. 7A). Exenatide also significantly increased expression of POMC mRNA by 2.4-fold, which was completely attenuated by the specific CREB inhibitor KG501 (25 μM) (Best et al., 2004) treated 1 hour earlier ($P < 0.05$, one-way ANOVA) (Fig. 7B).

We further confirmed whether CREB was a downstream acceptor of the cAMP/PKA signaling. Incubation with exenatide (10 nM) stimulated microglial CREB phosphorylation by 110%, which was completely blocked by the pretreatment (1 hour earlier) with H-89 (10 μM) ($P < 0.05$, one-way ANOVA) (Fig. 7C).

Finally, we determined whether CREB was activated by p38β. As shown in Fig. 7D, incubation of exenatide (10 nM) in cultured microglial cells significantly stimulated CREB phosphorylation, which was completely blocked by pretransfection (5 hours earlier) with siRNA/p38β, compared to the nonspecific oligo control ($P <$

0.05, one-way ANOVA). Distinctly, knockdown of p38α did not significantly alter exenatide-increased CREB phosphorylation.

Discussion

GLP-1R agonism by peptidic agonists GLP-1(7-36) and exenatide, non-peptidic agonist WB4-24 and iridoid agonists in herbal origin including catalpol and shanzhiside methylester, produced antinociception and neuroprotection through β-endorphin overexpression from the spinal cord and hippocampus (Fan et al., 2015; Fan et al., 2016; Gong et al., 2014b; Jia et al., 2015). Our current study further identified the cAMP/PKA/p38β/CREB signaling that mediated exenatide-induced microglial β-endorphin expression. Furthermore, we also revealed the antinociceptive role of p38β.

Although β-endorphin is expressed in neurons (Fichna et al., 2007), microglia (Fan et al., 2015), and astrocytes (Hauser et al., 1990), GLP-1R-induced β-endorphin expression occurs only in microglial cells originating either from the cortex (Fan et al., 2015), hippocampus (Jia et al., 2015) or spinal cord (Gong et al., 2014b). We further demonstrated co-expression of GLP-1Rs and β-endorphin in microglia. Moreover, treatment with exenatide concentration-dependently increased spinal POMC expression and β-endorphin release, with EC_{50} values of 4.1 and 7.5 nM, close to those for insulin expression in pancreatic islets (Baggio and Drucker, 2007). These results provide histological and functional couplings for the microglial GLP-1R/β-endorphin pathway.

The cAMP/PKA signaling through G_{as} has been identified as a classic pathway associated with GLP-1R-stimulated insulin expression in pancreatic β-cells (Koole et al., 2013). In this study, exenatide markedly increased intracellular cAMP levels and activated PKA, in parallel to POMC expression. Furthermore, pharmacological inhibition of cAMP production and PKA activation completely inhibited exenatide-increased POMC expression. Thus the cAMP/PKA signaling mediates GLP-1R-induced microglial POMC expression, along with GLP-1R-induced insulin

expression in pancreatic β-cells (Drucker et al., 1987).

Involvement of MAPKs in GLP-1R activation is complicated and controversial (Kawasaki et al., 2010; Lee et al., 2012; MacDonald et al., 2002). In our present study, activation of p38 (but not JNK1/2 or ERK1/2) mediated exenatide-induced p38 phosphorylation and POMC expression, which were totally blocked by the selective p38 but not JNK1/2 or ERK1/2 inhibitor. The results are consistent with our previous findings in which intrathecal the GLP-1R iridoid agonist shanzhiside methylester in neuropathic rats specifically stimulated spinal phosphorylation of p38 (but not JNK1/2 or ERK1/2) and expression of β-endorphin, which were entirely blocked by the p38 (but not ERK1/2 and JNK1/2) inhibitor (Fan et al., 2016). Collectively, p38 phosphorylation mediates exenatide-induced microglial POMC overexpression. Moreover, exenatide-induced p38 activation was nearly entirely reduced by H-89, indicating an upstream induction role of the cAMP/PKA signaling in p38 phosphorylation. The results are supported by previous findings in which p38 was activated following the cAMP-PKA signaling by activation of the family A of GPCRs such as β-adrenergic receptors (Hattori et al., 2016; Yamauchi et al., 1997; Yin et al., 2006).

A particularly compelling finding in this study is that p38β plays a crucial role in exenatide-induced microglial expression of β-endorphin and mechanical antiallodynia. Exenatide in primary microglia induced marked activation of total p38, shows no deviation from previous findings in pancreatic β-cells and Chinese hamster ovary cells (Macfarlane et al., 1997; Montrose-Rafizadeh et al., 1999). However, knockdown of p38β but not p38α completely attenuated exenatide-stimulated total p38 phosphorylation. Furthermore, intrathecal injection of exenatide also caused similar activation of p38 in contralateral and ipsilateral spinal cords. Consistent with the results in primary microglia, exenatide-induced total p38 phosphorylation in contralateral and ipsilateral spinal cords was completely blocked by the 7-day intrathecal siRNA/p38β, but not by siRNA/p38α. These results indirectly indicate that exenatide-stimulated phosphorylation of total p38 is entirely originated from the p38β isoform. Moreover, knockdown of p38β (but not p38α) also completely blocked

exenatide-increased POMC expression in primary microglia, and spinal POMC expression and mechanical antiallodynia in neuropathic rats. The results solidify our postulation that exenatide specifically induces spinal p38β phosphorylation, which subsequently mediates β-endorphin overexpression and antinociception. The broad impact of spinal p38β activation on endogenous opioid secretion and subsequent antinociception is supported by recent observations in which intrathecal siRNA/p38β blocked cynandione A- or bulleyaconitine A-induced spinal microglial total p38 activation and β-endorphin or dynorphin A expression, and spinal antinociception (Li et al., 2017; Huang et al., 2017).

It is interesting to note that partial knockdown of p38β (40-70% in our in vitro and in vivo settings) was able to fully inhibit exenatide-induced total p38 activation and POMC expression in primary microglia, and spinal POMC expression and mechanical antiallodynia in neuropathic rats. Although it is possible that our endpoints may not be sufficiently sensitive to distinguish the partial from the full inhibition, it is more likely that the remaining of p38β protein after RNA interference does not functionally serve to trigger the downstream signaling and, siRNA could just affect p38β levels by reducing the de novo and "active" form rather than the existing and "inactive" form. To surely illustrate the mechanisms, we need to perform spatial and temporal experiments using different concentrations of siRNA/p38β and exenatide to determine the minimal p38 protein level that is required for exenatide to execute biofunctions. Nevertheless, the separation phenomenon of knockdown of spinal microglial p38β has also been shown in formalin and substance P nociception (Svensson et al., 2005) and bulleyaconitine A (Li et al., 2017) and cynandione A antinociception (Huang et al., 2017). Moreover, partial knockdown of spinal GLP-1Rs, α3 glycine receptors or D-amino acid oxidase also completely inhibited their mediation of antinociception or nociception (Chen et al., 2012a; Gong et al., 2014b; Zhang et al., 2013).

In agreement with previous findings (Bachstetter et al., 2011; Xing et al., 2011), treatment with LPS in cultured primary microglia markedly activated p38 and dramatically stimulated expression of TNF-α, IL-6 and IL-1β, which were partially

attenuated by knockdown of p38α but not p38β, suggesting that LPS stimulated phosphorylation of p38 partially through p38α and the remaining activity may not be involved in p38β. The partial involvement of p38α on LPS-induced total p38 activation and overexpression of proinflammatory cytokines does not appear due to its partial knockdown, as nearly all the MAPK members are involved in LPS-induced microglial activation (Johnson and Lapadat, 2002; Nikodemova et al., 2006). Indeed, knockout/mutation of p38α (but not p38β) only partially reduced LPS-induced proinflammatory cytokine production (Li et al., 2008; O'Keefe et al., 2007; Xing et al., 2011). Hence, GLP-1R agonism by exenatide specifically activates p38β, which fully mediates POMC overexpression, whereas, in addition to other signaling molecules (but not p38β), LPS activates p38α, which partially induces overexpression of proinflammatory cytokines. The multitude of these results highlights differential roles of p38α and p38β in inflammation and nociception.

Belonging to the bZIP family transcription factors, CREB is a key transcription element for insulin gene expression after GLP-1R agonism (Dalle et al., 2011; Shaywitz and Greenberg, 1999). POMC expression was also stimulated by corticotrophin-releasing factor through the cAMP/PKA/CREB signaling in the anterior pituitary (Kraus and Hollt, 1995). We thus further detailed the involvement of CREB in regulation of exenatide-mediated POMC overexpression and its p38β-dependency. Exenatide stimulated CREB phosphorylation and mediated POMC overexpression, the latter of which was completely attenuated by the CREB inhibitor. Although PKA was originally identified to be a direct activator of CREB phosphorylation at the serine residue 133, ramification of the cAMP/PKA signaling is also involved in the diversity of signaling molecules including p38 (Dalle et al., 2011; Delghandi et al., 2005). In our study, exenatide-stimulated POMC overexpression was entirely attenuated by the p38 inhibitor and knockdown of p38β (but not p38α) and more specifically, exenatide-induced CREB phosphorylation was completely suppressed by silence of p38β but not p38α. Therefore, CREB phosphorylation is intermediated through p38β rather than direct PKA phosphorylation. Similar findings have been reported in which p38β and p38δ (but not p38α) were essential for

arsenite-stimulated CREB activation in the mouse epidermal cells (Che et al., 2013). Moreover, the blockade effect of H-89 also supports PKA-dependency for p38β to activate CREB. In summation, the Gs/cAMP/PKA/p38β/CREB signaling pathway entirely mediates GLP-1R-induced microglial β-endorphin overexpression and subsequent neuroprotection and antinociception (Fig. 8).

Spinal p38 activation induces overexpression of proinflammatory cytokines, which is associated with neuropathic pain (Ji et al., 2009; Ji and Suter, 2007). However, it is debated whether p38 and its isoforms could be targeted for the treatment of neuropathic pain (Galan-Arriero et al., 2014; Schafers et al., 2003). p38 inhibitors minocycline and SB203580 are generally not antinociceptive when neuropathy is established although they may be effective in preventing initiation of neuropathic pain (Fan et al., 2016; Mei et al., 2011; Schafers et al., 2003). p38 phosphorylation in the ipsilateral spinal cord was not significantly elevated in neuropathic rats approximately 14 days after peripheral nerve injury, which is supported by the previous finding that spinal p38 was phosphorylated between 5 hours and 3 days after spinal nerve ligation and its activation returned to baseline in 5 days (Schafers et al., 2003). Furthermore, the 7-day intrathecal either siRNA/p38α or siRNA/p38β did not alter withdrawal thresholds in ipsilateral paws. These findings support the notion that phosphorylation of p38 and its α or β isoform may not mediate nociception or antinociception in established neuropathy. However, silence of spinal p38β (but not p38α) by using the antisense oligonucleotides attenuated bone cancer pain, and formalin-, substance P- and carrageenan-induced tissue injury and inflammatory hyperalgesia (Dong et al., 2014; Fitzsimmons et al., 2010; Svensson et al., 2005). In contrast, systemic LPS-induced production of IL-1β and TNF-α was not altered by genetic knockout of p38β (O'Keefe et al., 2007; Xing et al., 2013). The reasons for the controversial findings are not known but they might be associated with different spinal p38β phosphorylation levels in these pain models at different stages.

Molecular Pharmacology Fast Forward. Published on February 15, 2017 as DOI: 10.1124/mol.116.107102
This article has not been copyedited and formatted. The final version may differ from this version.

Authorship Contributions

Participated in research design: Wang, Wu

Conducted experiments: Wu, Mao, Fan

Performed data analysis: Wu, Wang

Wrote or contributed to the writing of the manuscript: Wang, Wu

References

Bachstetter AD, Xing B, de Almeida L, Dimayuga ER, Watterson DM and Van Eldik LJ (2011) Microglial p38alpha MAPK is a key regulator of proinflammatory cytokine up-regulation induced by toll-like receptor (TLR) ligands or beta-amyloid (Abeta). *J Neuroinflam* **8**: 79.

Baggio LL and Drucker DJ (2007) Biology of incretins: GLP-1 and GIP. *Gastroenterology* **132**(6): 2131-2157.

Bennett BL, Sasaki DT, Murray BW, O'Leary EC, Sakata ST, Xu W, Leisten JC, Motiwala A, Pierce S, Satoh Y, Bhagwat SS, Manning AM and Anderson DW (2001) SP600125, an anthrapyrazolone inhibitor of Jun N-terminal kinase. *P Natl Acad Sci USA* **98**(24): 13681-13686.

Best JL, Amezcua CA, Mayr B, Flechner L, Murawsky CM, Emerson B, Zor T, Gardner KH and Montminy M (2004) Identification of small-molecule antagonists that inhibit an activator: coactivator interaction. *P Natl Acad Sci USA* **101**(51): 17622-17627.

Che X, Liu J, Huang H, Mi X, Xia Q, Li J, Zhang D, Ke Q, Gao J and Huang C (2013) p27 suppresses cyclooxygenase-2 expression by inhibiting p38beta and p38delta-mediated CREB phosphorylation upon arsenite exposure. *Biochimica et biophysica acta* **1833**(9): 2083-2091.

Chen XL, Li XY, Qian SB, Wang YC, Zhang PZ, Zhou XJ and Wang YX (2012a) Down-regulation of spinal D-amino acid oxidase expression blocks formalin-induced tonic pain. *Biochem Bioph Res Co* **421**(3): 501-507.

Chen Y, Huang X, Zhang YW, Rockenstein E, Bu G, Golde TE, Masliah E and Xu H (2012b) Alzheimer's beta-secretase (BACE1) regulates the cAMP/PKA/CREB pathway independently of beta-amyloid. *J Neurosci* **32**(33): 11390-11395.

Chijiwa T, Mishima A, Hagiwara M, Sano M, Hayashi K, Inoue T, Naito K, Toshioka T and Hidaka H (1990) Inhibition of forskolin-induced neurite outgrowth and protein phosphorylation by a newly synthesized selective inhibitor of cyclic AMP-dependent protein kinase, N-[2-(p-bromocinnamylamino)ethyl]-5-isoquinolinesulfonamide (H-89), of PC12D pheochromocytoma cells. *J Biol Chem* **265**(9): 5267-5272.

Coulthard LR, White DE, Jones DL, McDermott MF and Burchill SA (2009) p38(MAPK): stress responses from molecular mechanisms to therapeutics. *Trends Mol Med* **15**(8): 369-379.

Dalle S, Quoyer J, Varin E and Costes S (2011) Roles and regulation of the transcription factor CREB in pancreatic beta -cells. *Curr Mol Pharmacol* **4**(3): 187-195.

Delghandi MP, Johannessen M and Moens U (2005) The cAMP signalling pathway activates CREB through PKA, p38 and MSK1 in NIH 3T3 cells. *Cell Signal* **17**(11): 1343-1351.

DeSilva DR, Jones EA, Favata MF, Jaffee BD, Magolda RL, Trzaskos JM and Scherle PA (1998) Inhibition of mitogen-activated protein kinase kinase blocks T cell proliferation but does not induce or prevent anergy. *J Immunol* **160**(9): 4175-4181.

Dong H, Xiang HB, Ye DW and Tian XB (2014) Inhibitory effects of intrathecal p38beta antisense oligonucleotide on bone cancer pain in rats. *Int J Clin Exp Patho* **7**(11): 7690-7698.

Drucker DJ, Philippe J, Mojsov S, Chick WL and Habener JF (1987) Glucagon-like peptide I stimulates insulin gene expression and increases cyclic AMP levels in a rat islet cell line. *P Natl Acad Sci USA* **84**(10): 3434-3438.

Engh RA, Girod A, Kinzel V, Huber R and Bossemeyer D (1996) Crystal structures of catalytic subunit of cAMP-dependent protein kinase in complex with isoquinolinesulfonyl protein kinase inhibitors H7, H8, and H89. Structural implications for selectivity. *J Biol Chem* **271**(42): 26157-26164.

Fan H, Gong N, Li TF, Ma AN, Wu XY, Wang MW and Wang YX (2015) The non-peptide GLP-1 receptor agonist WB4-24 blocks inflammatory nociception by stimulating beta-endorphin release from spinal microglia. *Brit J Pharmacol* **172**(1): 64-79.

Fan H, Li TF, Gong N and Wang YX (2016) Shanzhiside methylester, the principle effective iridoid glycoside from the analgesic herb Lamiophlomis rotata, reduces neuropathic pain by stimulating spinal microglial beta-endorphin expression. *Neuropharmacology* **101**: 98-109.

Fichna J, Janecka A, Costentin J and Do Rego JC (2007) The endomorphin system and its evolving neurophysiological role. *Pharmacol Rev* **59**(1): 88-123.

Fitzsimmons BL, Zattoni M, Svensson CI, Steinauer J, Hua XY and Yaksh TL (2010) Role of spinal p38alpha and beta MAPK in inflammatory hyperalgesia and spinal COX-2 expression. *Neuroreport* **21**(4): 313-317.

Galan-Arriero I, Avila-Martin G, Ferrer-Donato A, Gomez-Soriano J, Bravo-Esteban E and Taylor J (2014) Oral administration of the p38alpha MAPK inhibitor, UR13870, inhibits affective pain behavior after spinal cord injury. *Pain* **155**(10): 2188-2198.

Gong N, Fan H, Ma AN, Xiao Q and Wang YX (2014a) Geniposide and its iridoid analogs exhibit antinociception by acting at the spinal GLP-1 receptors. *Neuropharmacology* **84**: 31-45.

Gong N, Xiao Q, Zhu B, Zhang CY, Wang YC, Fan H, Ma AN and Wang YX (2014b) Activation of spinal glucagon-like peptide-1 receptors specifically suppresses pain hypersensitivity. *J Neurosci* **34**(15): 5322-5334.

Graaf C, Donnelly D, Wootten D, Lau J, Sexton PM, Miller LJ, Ahn JM, Liao J, Fletcher MM, Yang D, Brown AJ, Zhou C, Deng J and Wang MW (2016) Glucagon-Like Peptide-1 and Its Class B G Protein-Coupled Receptors: A Long March to Therapeutic Successes. *Pharmacol Rev* **68**(4): 954-1013.

Hallbrink M, Holmqvist T, Olsson M, Ostenson CG, Efendic S and Langel U (2001) Different domains in the third intracellular loop of the GLP-1 receptor are responsible for Galpha(s) and Galpha(i)/Galpha(o) activation. *Biochim Biophys Acta* **1546**(1): 79-86.

Hansen HH, Fabricius K, Barkholt P, Niehoff ML, Morley JE, Jelsing J, Pyke C, Knudsen LB, Farr SA and Vrang N (2015) The GLP-1 Receptor Agonist Liraglutide Improves Memory Function and Increases Hippocampal CA1

Neuronal Numbers in a Senescence-Accelerated Mouse Model of Alzheimer's Disease. *J Alzheimers Dis* **46**(4): 877-888.

Harkavyi A and Whitton PS (2010) Glucagon-like peptide 1 receptor stimulation as a means of neuroprotection. *Brit J Pharmacol* **159**(3): 495-501.

Hattori K, Naguro I, Okabe K, Funatsu T, Furutani S, Takeda K and Ichijo H (2016) ASK1 signalling regulates brown and beige adipocyte function. *Nature communications* **7**: 11158.

Hauser KF, Osborne JG, Stiene-Martin A and Melner MH (1990) Cellular localization of proenkephalin mRNA and enkephalin peptide products in cultured astrocytes. *Brain Res* **522**(2): 347-353.

Holscher C (2012) Potential role of glucagon-like peptide-1 (GLP-1) in neuroprotection. *CNS drugs* **26**(10): 871-882.

Holz GG, Leech CA, Heller RS, Castonguay M and Habener JF (1999) cAMP-dependent mobilization of intracellular Ca2+ stores by activation of ryanodine receptors in pancreatic beta-cells. A Ca2+ signaling system stimulated by the insulinotropic hormone glucagon-like peptide-1-(7-37). *J Biol Chem* **274**(20): 14147-14156.

Holz GGt, Leech CA and Habener JF (1995) Activation of a cAMP-regulated Ca(2+)-signaling pathway in pancreatic beta-cells by the insulinotropic hormone glucagon-like peptide-1. *J Biol Chem* **270**(30): 17749-17757.

Huang Q, Mao XF, Sun ML, Wu HY, Wang X and Wang YX (2017). Cynandione A attenuates neuropathic pain through p38β MAPK-mediated spinal microglial expression of β-endorphin. *Brain Behav. Immun.*, under review.

Ji RR, Gereau RWt, Malcangio M and Strichartz GR (2009) MAP kinase and pain. *Brain Res Rev* **60**(1): 135-148.

Ji RR and Suter MR (2007) p38 MAPK, microglial signaling, and neuropathic pain. *Mol Pain* **3**: 33.

Jia Y, Gong N, Li TF, Zhu B and Wang YX (2015) Peptidic exenatide and herbal catalpol mediate neuroprotection via the hippocampal GLP-1 receptor/beta-endorphin pathway. *Pharmacol Res* **102**: 276-285.

Johnson GL and Lapadat R (2002) Mitogen-activated protein kinase pathways mediated by ERK, JNK, and p38 protein kinases. *Science* **298**(5600): 1911-1912.

Kawasaki Y, Harashima S, Sasaki M, Mukai E, Nakamura Y, Harada N, Toyoda K, Hamasaki A, Yamane S, Yamada C, Yamada Y, Seino Y and Inagaki N (2010) Exendin-4 protects pancreatic beta cells from the cytotoxic effect of rapamycin by inhibiting JNK and p38 phosphorylation. *Horm Metab Res* **42**(5): 311-317.

Kemp DM and Habener JF (2001) Insulinotropic hormone glucagon-like peptide 1 (GLP-1) activation of insulin gene promoter inhibited by p38 mitogen-activated protein kinase. *Endocrinology* **142**(3): 1179-1187.

Kim S, Moon M and Park S (2009) Exendin-4 protects dopaminergic neurons by inhibition of microglial activation and matrix metalloproteinase-3 expression in an animal model of Parkinson's disease. *J Endocrinol* **202**(3): 431-439.

Kim SH and Chung JM (1992) An experimental model for peripheral neuropathy produced by segmental spinal nerve ligation in the rat. *Pain* **50**(3): 355-363.

Koole C, Pabreja K, Savage EE, Wootten D, Furness SG, Miller LJ, Christopoulos A and Sexton PM (2013) Recent advances in understanding GLP-1R (glucagon-like peptide-1 receptor) function. *Biochem Soc T* **41**(1): 172-179.

Koole C, Wootten D, Simms J, Valant C, Sridhar R, Woodman OL, Miller LJ, Summers RJ, Christopoulos A and Sexton PM (2010) Allosteric ligands of the glucagon-like peptide 1 receptor (GLP-1R) differentially modulate endogenous and exogenous peptide responses in a pathway-selective manner: implications for drug screening. *Mol Pharmacol* **78**(3): 456-465.

Kraus J and Hollt V (1995) Identification of a cAMP-response element on the human proopiomelanocortin gene upstream promoter. *DNA Cell Biol* **14**(2): 103-110.

Lali FV, Hunt AE, Turner SJ and Foxwell BM (2000) The pyridinyl imidazole inhibitor SB203580 blocks phosphoinositide-dependent protein kinase activity, protein kinase B phosphorylation, and retinoblastoma hyperphosphorylation in interleukin-2-stimulated T cells independently of p38 mitogen-activated protein kinase. *J Biol Chem* **275**(10): 7395-7402.

Lee YS and Jun HS (2014) Anti-diabetic actions of glucagon-like peptide-1 on pancreatic beta-cells. *Metabolism* **63**(1): 9-19.

Lee YS, Park MS, Choung JS, Kim SS, Oh HH, Choi CS, Ha SY, Kang Y, Kim Y and Jun HS (2012) Glucagon-like peptide-1 inhibits adipose tissue macrophage infiltration and inflammation in an obese mouse model of diabetes. *Diabetologia* **55**(9): 2456-2468.

Li Q, Zhang N, Zhang D, Wang Y, Lin T, Wang Y, Zhou H, Ye Z, Zhang F, Lin SC and Han J (2008) Determinants that control the distinct subcellular localization of p38alpha-PRAK and p38beta-PRAK complexes. *J Biol Chem* **283**(16): 11014-11023.

Li TF, Wu HY, Wang YR and Wang YX (2017). Molecular signaling underlying bulleyaconitine A (BAA)-induced microglial expression of prodynorphin. *Sci. Rep.*, under review.

Liu J, Chen L, zhou Y, Liu X and Tang K (2014) Insulin-like growth factor-1 and bone morphogenetic protein-2 jointly mediate prostaglandin E2-induced adipogenic differentiation of rat tendon stem cells. *PloS one* **9**(1): e85469.

Liu L, Cao Z, Chen J, Li R, Cao Y, Zhu C, Wu K, Wu J, Liu F and Zhu Y (2012) Influenza A virus induces interleukin-27 through cyclooxygenase-2 and protein kinase A signaling. *J Biol Chem* **287**(15): 11899-11910.

MacDonald PE, El-Kholy W, Riedel MJ, Salapatek AM, Light PE and Wheeler MB (2002) The multiple actions of GLP-1 on the process of glucose-stimulated insulin secretion. *Diabetes* **51** Suppl 3: S434-442.

Macfarlane WM, Smith SB, James RF, Clifton AD, Doza YN, Cohen P and Docherty K (1997) The p38/reactivating kinase mitogen-activated protein kinase cascade mediates the activation of the transcription factor insulin upstream factor 1 and insulin gene transcription by high glucose in pancreatic beta-cells. *J Biol Chem* **272**(33): 20936-20944.

Mei XP, Xu H, Xie C, Ren J, Zhou Y, Zhang H and Xu LX (2011) Post-injury administration of minocycline: an effective treatment for nerve-injury induced neuropathic pain. *Neurosci Res* **70**(3): 305-312.

Milligan ED and Watkins LR (2009) Pathological and protective roles of glia in chronic pain. *Nat Rev Neurosci* **10**(1): 23-36.

Mitsuya H, Jarrett RF, Matsukura M, Di Marzo Veronese F, DeVico AL, Sarngadharan MG, Johns DG, Reitz MS and Broder S (1987) Long-term inhibition of human T-lymphotropic virus type III/lymphadenopathy-associated virus (human immunodeficiency virus) DNA synthesis and RNA expression in T cells protected by 2',3'-dideoxynucleosides in vitro. *P Natl Acad Sci USA* **84**(7): 2033-2037.

Montrose-Rafizadeh C, Avdonin P, Garant MJ, Rodgers BD, Kole S, Yang H, Levine MA, Schwindinger W and Bernier M (1999) Pancreatic glucagon-like peptide-1 receptor couples to multiple G proteins and activates mitogen-activated protein kinase pathways in Chinese hamster ovary cells. *Endocrinology* **140**(3): 1132-1140.

Nikodemova M, Duncan ID and Watters JJ (2006) Minocycline exerts inhibitory effects on multiple mitogen-activated protein kinases and IkappaBalpha degradation in a stimulus-specific manner in microglia. *J Neurochem* **96**(2): 314-323.

O'Keefe SJ, Mudgett JS, Cupo S, Parsons JN, Chartrain NA, Fitzgerald C, Chen SL, Lowitz K, Rasa C, Visco D, Luell S, Carballo-Jane E, Owens K and Zaller DM (2007) Chemical genetics define the roles of p38alpha and p38beta in acute and chronic inflammation. *J Biol Chem* **282**(48): 34663-34671.

Pyo H, Joe E, Jung S, Lee SH and Jou I (1999) Gangliosides activate cultured rat brain microglia. *J Biol Chem* 274(49): 34584-34589.

Raghavendra V, Tanga FY and DeLeo JA (2004) Complete Freunds adjuvant-induced peripheral inflammation evokes glial activation and proinflammatory cytokine expression in the CNS. *Eur J Neurosci* **20**(2): 467-473.

Schafers M, Svensson CI, Sommer C and Sorkin LS (2003) Tumor necrosis factor-alpha induces mechanical allodynia after spinal nerve ligation by activation of p38 MAPK in primary sensory neurons. *J Neurosci* **23**(7): 2517-2521.

Shaywitz AJ and Greenberg ME (1999) CREB: a stimulus-induced transcription factor activated by a diverse array of extracellular signals. *Annu Rev Biochem* **68**: 821-861.

Si H and Liu D (2009) Isoflavone genistein protects human vascular endothelial cells against tumor necrosis factor-alpha-induced apoptosis through the p38beta mitogen-activated protein kinase. *Apoptosis* **14**(1): 66-76.

Sitte N, Busch M, Mousa SA, Labuz D, Rittner H, Gore C, Krause H, Stein C and Schafer M (2007) Lymphocytes upregulate signal sequence-encoding proopiomelanocortin mRNA and beta-endorphin during painful inflammation in vivo. *J Neuroimmunol* **183**(1-2): 133-145.

Svensson CI, Fitzsimmons B, Azizi S, Powell HC, Hua XY and Yaksh TL (2005) Spinal p38beta isoform mediates tissue injury-induced hyperalgesia and spinal sensitization. *J Neurochem* **92**(6): 1508-1520.

Wang Y, Huang S, Sah VP, Ross J, Jr., Brown JH, Han J and Chien KR (1998) Cardiac muscle cell hypertrophy and apoptosis induced by distinct members of the p38 mitogen-activated protein kinase family. *J Biol Chem* **273**(4): 2161-2168.

Wang YX and Pang CC (1993) Functional integrity of the central and sympathetic nervous systems is a prerequisite for pressor and tachycardic effects of diphenyleneiodonium, a novel inhibitor of nitric oxide synthase. *J Pharmacol Exp Ther* **265**: 263-272.

Wei H, Wu HY, Fan H, Li TF, Ma AN, Li XY, Wang YX and Pertovaara A (2016) Potential role of spinal TRPA1 channels in antinociceptive tolerance to spinally administered morphine. *Pharmacol Rep* **68**(2): 472-475.

Xing B, Bachstetter AD and Van Eldik LJ (2011) Microglial p38alpha MAPK is critical for LPS-induced neuron degeneration, through a mechanism involving TNFalpha. *Mol Neurodegener* **6**: 84.

Xing B, Bachstetter AD and Van Eldik LJ (2013) Deficiency in p38beta MAPK fails to inhibit cytokine production or protect neurons against inflammatory insult in

in vitro and in vivo mouse models. *PloS one* **8**(2): e56852.

Xu M, Wu HY, Liu H, Gong N, Wang YR, Wang YX (2017). Morroniside, a secoiridoid glycoside from *Cornus officinalis,* attenuates neuropathic pain by activation of spinal glucagon-like peptide-1 receptors. *Br. J. Pharmacol.* DOI: 10.1111/bph.13720.

Yamauchi J, Nagao M, Kaziro Y and Itoh H (1997) Activation of p38 mitogen-activated protein kinase by signaling through G protein-coupled receptors. Involvement of Gbetagamma and Galphaq/11 subunits. *J Biol Chem* **272**(44): 27771-27777.

Yang Y, Zhu X, Chen Y, Wang X and Chen R (2007) p38 and JNK MAPK, but not ERK1/2 MAPK, play important role in colchicine-induced cortical neurons apoptosis. *Eur J Pharmacol* **576**(1-3): 26-33.

Yin F, Wang YY, Du JH, Li C, Lu ZZ, Han C and Zhang YY (2006) Noncanonical cAMP pathway and p38 MAPK mediate beta2-adrenergic receptor-induced IL-6 production in neonatal mouse cardiac fibroblasts. *J Mol Cell Cardiol* **40**(3): 384-393.

Zhang JY, Gong N, Huang JL, Guo LC and Wang YX (2013) Gelsemine, a principal alkaloid from Gelsemium sempervirens Ait., exhibits potent and specific antinociception in chronic pain by acting at spinal alpha3 glycine receptors. *Pain* **154**(11): 2452-2462.

Zhu B, Gong N, Fan H, Peng CS, Ding XJ, Jiang Y and Wang YX (2014) Lamiophlomis rotata, an orally available Tibetan herbal painkiller, specifically reduces pain hypersensitivity states through the activation of spinal glucagon-like peptide-1 receptors. *Anesthesiology* **121**(4): 835-851.

Molecular Pharmacology Fast Forward. Published on February 15, 2017 as DOI: 10.1124/mol.116.107102
This article has not been copyedited and formatted. The final version may differ from this version.

Footnotes

This study was supported in part by grants from the National Natural Science Foundation of China [No.81374000] and the Shanghai Industrial Translational Project [No. 15401901300].

Molecular Pharmacology Fast Forward. Published on February 15, 2017 as DOI: 10.1124/mol.116.107102
This article has not been copyedited and formatted. The final version may differ from this version.

Figure legends

Fig. 1. Representative photomicrographs of expression of the glucagon-like peptide-1 receptor (GLP-1R) and β-endorphin in primary microglia (**A**-**L**), and stimulatory effects of exenatide on the β-endorphin precursor gene (POMC) expression (**M**) and β-endorphin release (**N**) in primary cultures of microglia. Primary microglial cells were collected from the cortex of 1-day-old neonatal rats. For the immunostaining study, double immunofluorescence staining of GLP-1R and IBA-1 (**A**-**D**), β-endorphin and IBA-1 (**E**-**H**), and β-endorphin and GLP-1R (**I**-**L**) were performed, and DAPI staining was used to identify cell nuclei. Scale bars: 25 μM. For the stimulatory effect of exenatide, incubation of exenatide in gradient concentrations (0.3, 1, 3, 10, 30, and 100 nM) with cultured primary microglial cells for 2 hours. POMC expression in microglia and β-endorphin levels in the microglial cultural medium were determined by using real-time quantitative PCR and a commercial fluorescent immunoassay kit, respectively. Data are presented as means ± SD (N=3 in each treatment).

Fig. 2. Stimulatory effects of exenatide on intracellular cAMP levels **(A)** and PKA phosphorylation (**B**), and blockade effects of the adenylate cyclase inhibitor DDA (**C**) and PKA inhibitor H-89 (**D**) on exenatide-stimulated β-endorphin overexpression in primary cultures of microglia. Primary microglial cells were collected from the cortex of 1-day-old neonatal rats. For cAMP and *p*-PKA measurements, exenatide was incubated with cultured primary microglia for 30 minutes. The intracellular cAMP level and *p*-PKA expression were measured using the fluorescent immunoassay kit and western blotting, respectively. The representative gels are inserted at the top of the figure. For the blockade effects, DDA (100 μM) and H89 (10 μM) were incubated with microglia for 1 hour before exenatide (10 nM) treatment. Two hours later, POMC gene expression was determined by real-time quantitative PCR. Data are means ± SD (N=3-4 in each treatment). * and # denote statistically significant differences compared to the control and exenatide treatment group, respectively (P <

0.05, unpaired and two-tailed Student t-test and one-way ANOVA followed by post-hoc SNK tests, respectively).

Fig. 3. Stimulatory effects of exenatide on phosphorylation of p38 (**A**), ERK1/2 (**B**) and JNK1/2 MAPK (**C**), and blockade effects of the p38 inhibitor SB203580 (**D**), ERK1/2 inhibitor U0126 (**E**), JNK1/2 inhibitor SP600125 (**F**) and the PKA inhibitor H-89 (**G**) on exenatide-increased p38 phosphorylation and POMC mRNA expression in primary cultures of microglia. Primary microglial cells were collected from the cortex of 1-day-old neonatal rats. For the MAPKs phosphorylation measurement, exenatide (10 nM) was incubated with microglia for 15, 30 and 60 minutes and phosphorylation of p38, ERK1/2 and JNK1/2 was determined using western blotting. For the blockade effects, SB203580 (50 μM), U0126 (50 μM), SP600125 (50 μM) and H89 (10 μM) were incubated with microglia 1 hour before exenatide (10 nM) treatment. 0.5 or 2 hours later, p38 phosphorylation or POMC mRNA expression was determined using western blotting or real-time quantitative PCR. Data are means ± SD (N=3 in each treatment), and the representative gels are inserted in their respective figures. * and $^{\#}$ denote statistically significant differences compared to the control and exenatide treatment group, respectively ($P < 0.05$, one-way ANOVA followed by post-hoc SNK tests).

Fig 4. Blockade effects of siRNA/p38α and siRNA/p38β on p38α (**A, B**) and p38β(**C**, **D**) gene and protein expression, exenatide-increased p38 phosphorylation (**E**) and β-endorphin gene expression (**F**). Primary microglial cells were collected from the cortex of 1-day-old neonatal rats. For the gene silencing study, the equal concentration (5 μg/mL) of siRNA/p38α, siRNA/p38β and the nonspecific oligos were transfected with microglia by using DOTAP for 5 hours. p38α and p38β gene and protein expressions were determined by using real-time quantitative PCR and western blotting, respectively, after further 24 hours interference. For the blockade effects, siRNA/p38α and siRNA/p38β interference was performed in cultured microglia for 24 hours before exenatide (10 nM) challenge. p38 phosphorylation or expression of

POMC was analyzed 0.5 or 2 hours after exenatide treatments by western blotting or real-time quantitative PCR. Data are means ± SD (N=3-4 in each treatment), and the representative gels are inserted in their respective figures. * and # denote statistically significant differences compared to the control and exenatide or LPS treatment group, respectively ($P < 0.05$, one-way ANOVA followed by post-hoc SNK tests).

Fig. 5. Blockade effects of siRNA/p38α and siRNA/p38β on LPS-increased p38 phosphorylation (**A**) and expression of TNF-α (**B**), IL-1β (**C**) and IL-6 (**D**). Primary microglial cells were collected from the cortex of 1-day-old neonatal rats. For the gene silencing study, the equal concentration (5 μg/mL) of siRNA/p38α, siRNA/p38β and the nonspecific oligos were transfected with microglia by using DOTAP for 5 hours. For the blockade effects, siRNA/p38α and siRNA/p38β interferences were performed in cultured microglia for 24 hours before LPS (10 ng) challenge. p38 phosphorylation or expression of proinflammatory cytokines was analyzed 0.5 or 2 hours after LPS treatment by western blotting or real-time quantitative PCR. Data are means ± SD (N=3-5 in each treatment), and the representative gels are inserted in their respective figures. * and # denote statistically significant differences compared to the control and exenatide or LPS treatment group, respectively ($P < 0.05$, one-way ANOVA followed by post-hoc SNK tests).

Fig. 6. Effects of multiple-daily intrathecal injections of siRNA/p38α and siRNA/p38β MAPK on baseline paw withdrawal thresholds (**A**), exenatide-induced antinociception (**B**), spinal p38α (**C** and **D**) and p38β (**E** and **F)** gene and protein expression, and exenatide-induced spinal p38 phosphorylation (**G** and **H**) and POMC expression (**I**) in established neuropathic rats. Rats received multiple-daily intrathecal injections of the vehicle (DOTAP, 40 μg/day), nonspecific oligos (5 μg/day), siRNA/p38α (5 μg/day) and siRNA/p38β (5 μg/day) for 7 days. The baseline paw withdrawal thresholds were measured once daily by using electronic von frey filaments. On the eighth day, a single bolus of exenatide (100 ng) was intrathecally injected and mechanical nociceptive behaviors were quantified 1 hour after injection.

Spinal lumbar enlargements were immediately obtained after completion of behavioral assessments. Expression of p38α, p38β and POMC mRNA, levels of p38α and p38β protein, and phosphorylation p38 were determined by using real-time quantitative PCR and western blotting, respectively. Data are means ± SD (N=5-6 in each group) and the representative gels are inserted in their respective figures. * and # denote statistically significant differences compared to the control and exenatide group, respectively ($P < 0.05$, one-way ANOVA followed by post-hoc SNK tests).

Fig. 7. Stimulatory effects of exenatide on CREB phosphorylation (**A**), and blockade effects of the CREB inhibitor KG501on exenatide-induced β-endorphin gene (POMC) overexpression (**B**), and PKA inhibitor H-89 (**C**) and gene silencers siRNA/p38α and siRNA/p38β (**D**) on exenatide-stimulated CREB phosphorylation in primary cultures of microglia. Primary microglial cells were isolated from the cortex of 1-day-old neonatal rats. For CREB phosphorylation, incubation of exenatide (10 nM) with microglial cells for 30 minutes and CREB phosphorylation was determined using western blotting. For the blockade effects, KG501 (25 μM) and H-89 (10 μM), or siRNA/p38α (5 μg/mL) and siRNA/p38β (5 μg/mL) in a formulation with the transfection reagent (DOTAP, 50 μM) were incubated with microglial cells 1 or 24 hours before exenatide (10 nM) treatment. CREB phosphorylation or POMC expression was analyzed by using western blotting or real-time quantitative PCR. Data are means ± SD (N=3-4 in each treatment) and the representative gels are inserted in their respective figures. * and # denote statistically significant differences compared to the control and exenatide treatment, respectively ($P < 0.05$, unpaired and two-tailed Student t-test and one-way ANOVA followed by post-hoc SNK test).

Fig. 8. Proposed signal transduction pathways for the glucagon-like peptide-1 receptor (GLP-1R)- and TLR4 receptor-induced expressions of β-endorphin and proinflammatory cytokines in microglia. Following agonism of GLP-1Rs, the cAMP/PKA, p38β (but not p38α) MAPK and CREB signals are successively activated which mediate β-endorphin expression and subsequent neuroprotection and

antinociception (blue lines). On the other hand, p38α MAPK and NF-κB signals are successively activated following agonism of TLR4 receptors by LPS, which partially mediate expression of proinflammatory factors including TNF-α, IL-1β and IL-6 and subsequent nociception (black line).

Molecular Pharmacology Fast Forward. Published on February 15, 2017 as DOI: 10.1124/mol.116.107102
This article has not been copyedited and formatted. The final version may differ from this version.

Figure 1

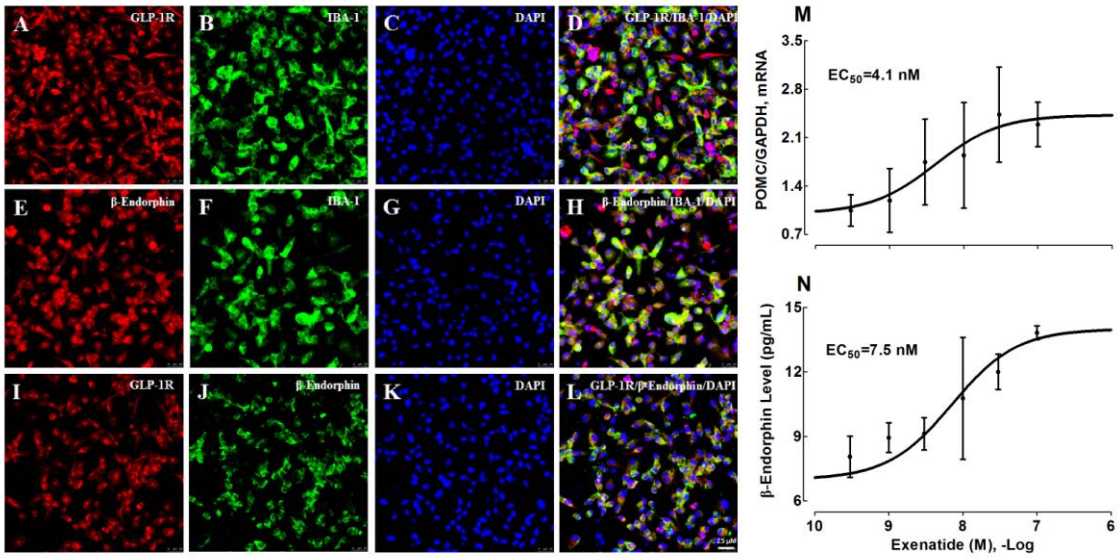

Molecular Pharmacology Fast Forward. Published on February 15, 2017 as DOI: 10.1124/mol.116.107102
This article has not been copyedited and formatted. The final version may differ from this version.

Figure 2

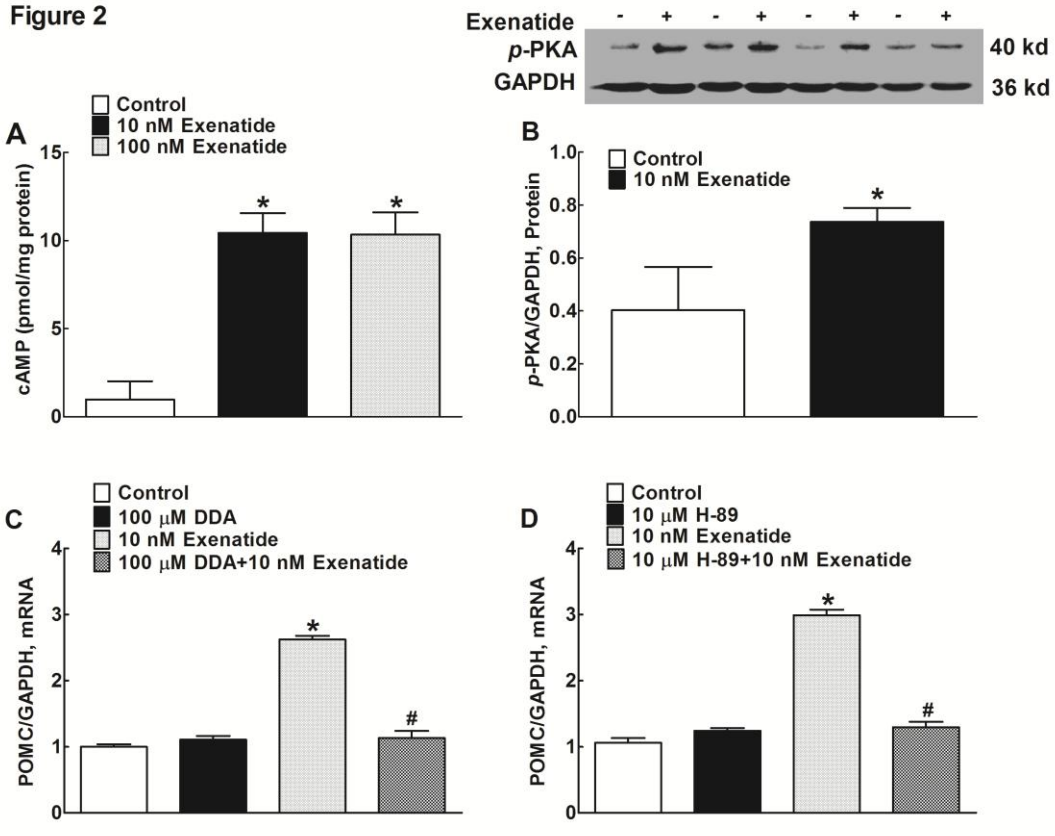

Molecular Pharmacology Fast Forward. Published on February 15, 2017 as DOI: 10.1124/mol.116.107102
This article has not been copyedited and formatted. The final version may differ from this version.

Figure 3

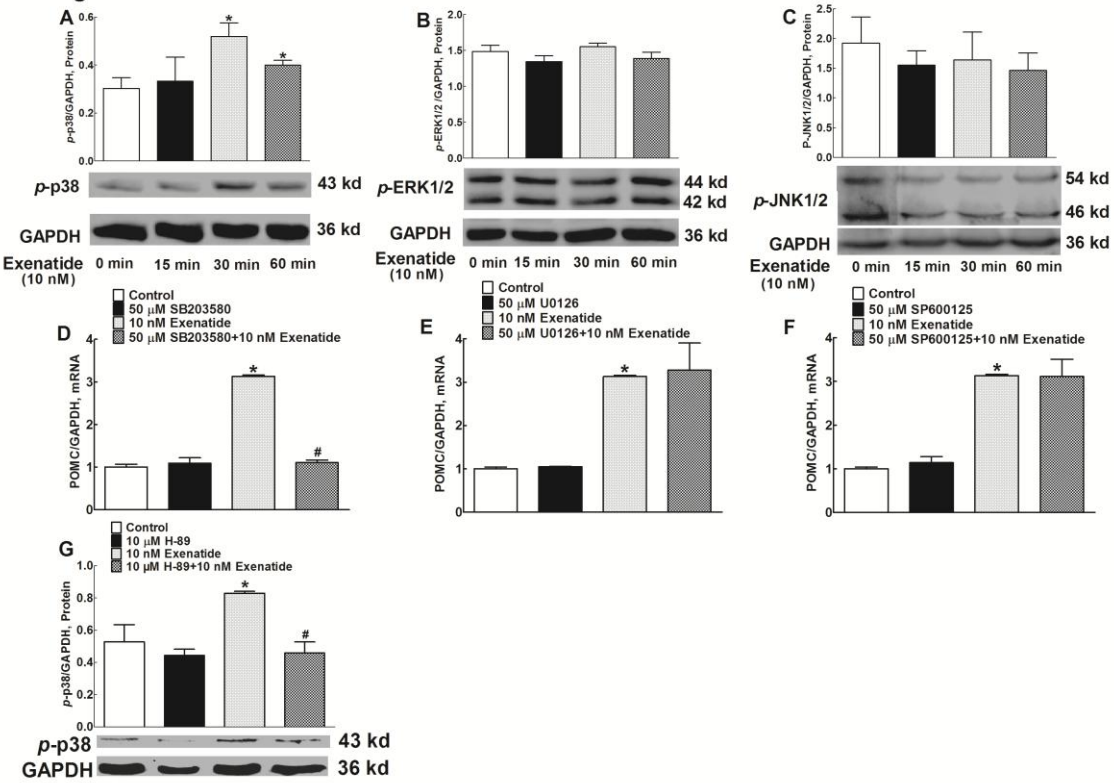

Molecular Pharmacology Fast Forward. Published on February 15, 2017 as DOI: 10.1124/mol.116.107102
This article has not been copyedited and formatted. The final version may differ from this version.

Figure 4

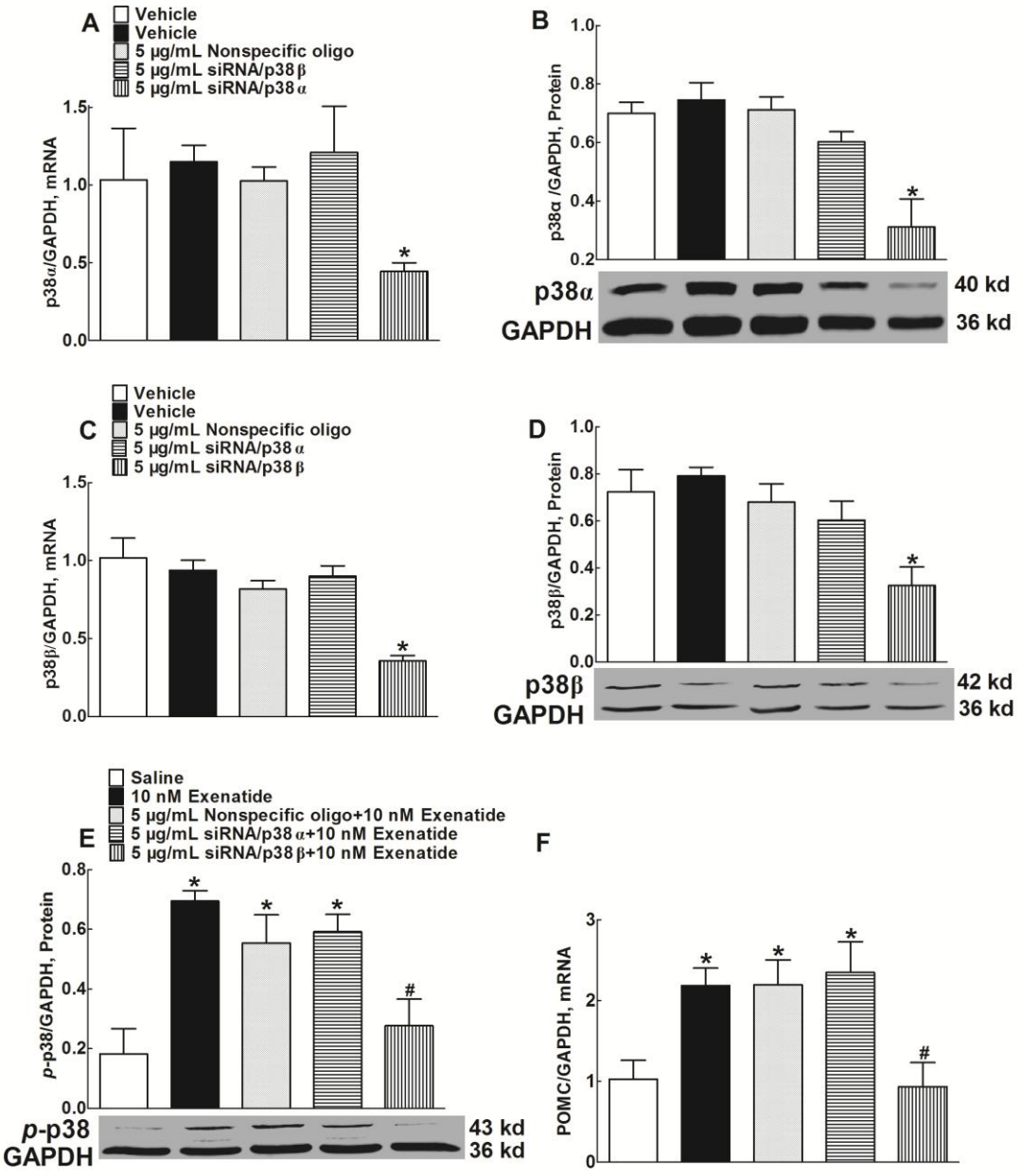

Molecular Pharmacology Fast Forward. Published on February 15, 2017 as DOI: 10.1124/mol.116.107102
This article has not been copyedited and formatted. The final version may differ from this version.

Figure 5

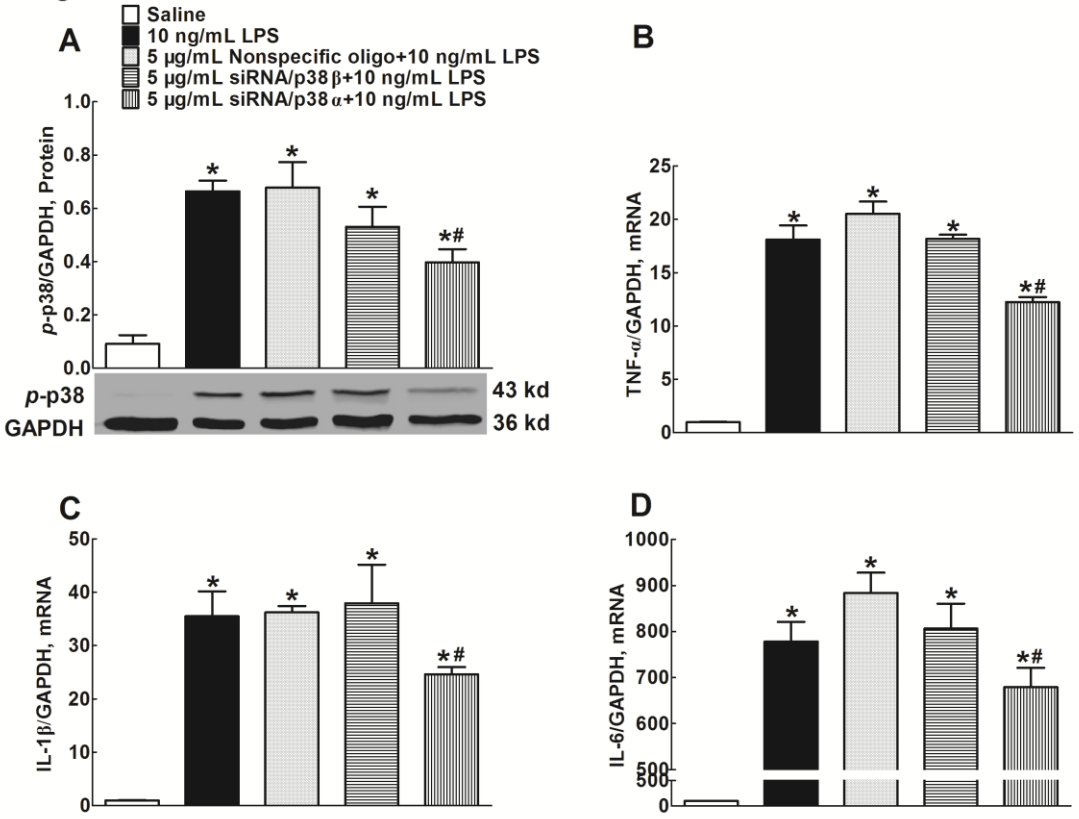

Molecular Pharmacology Fast Forward. Published on February 15, 2017 as DOI: 10.1124/mol.116.107102
This article has not been copyedited and formatted. The final version may differ from this version.

Figure 6

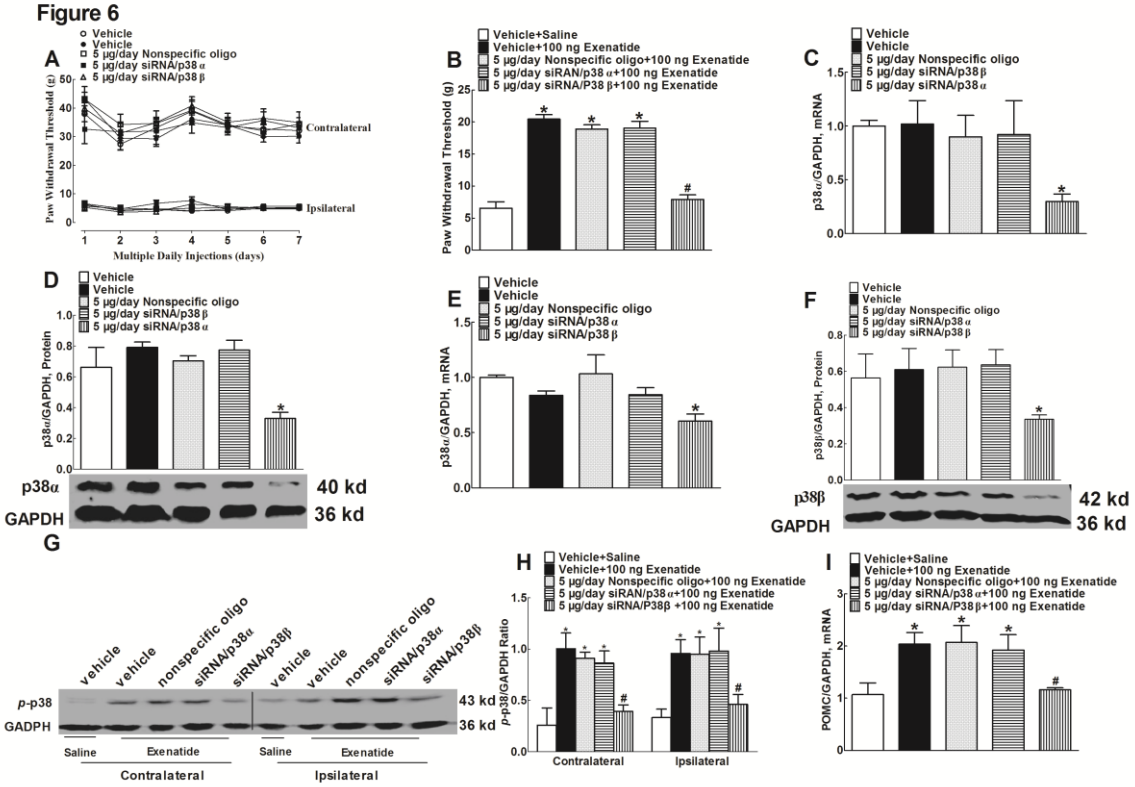

Molecular Pharmacology Fast Forward. Published on February 15, 2017 as DOI: 10.1124/mol.116.107102
This article has not been copyedited and formatted. The final version may differ from this version.

Figure 7

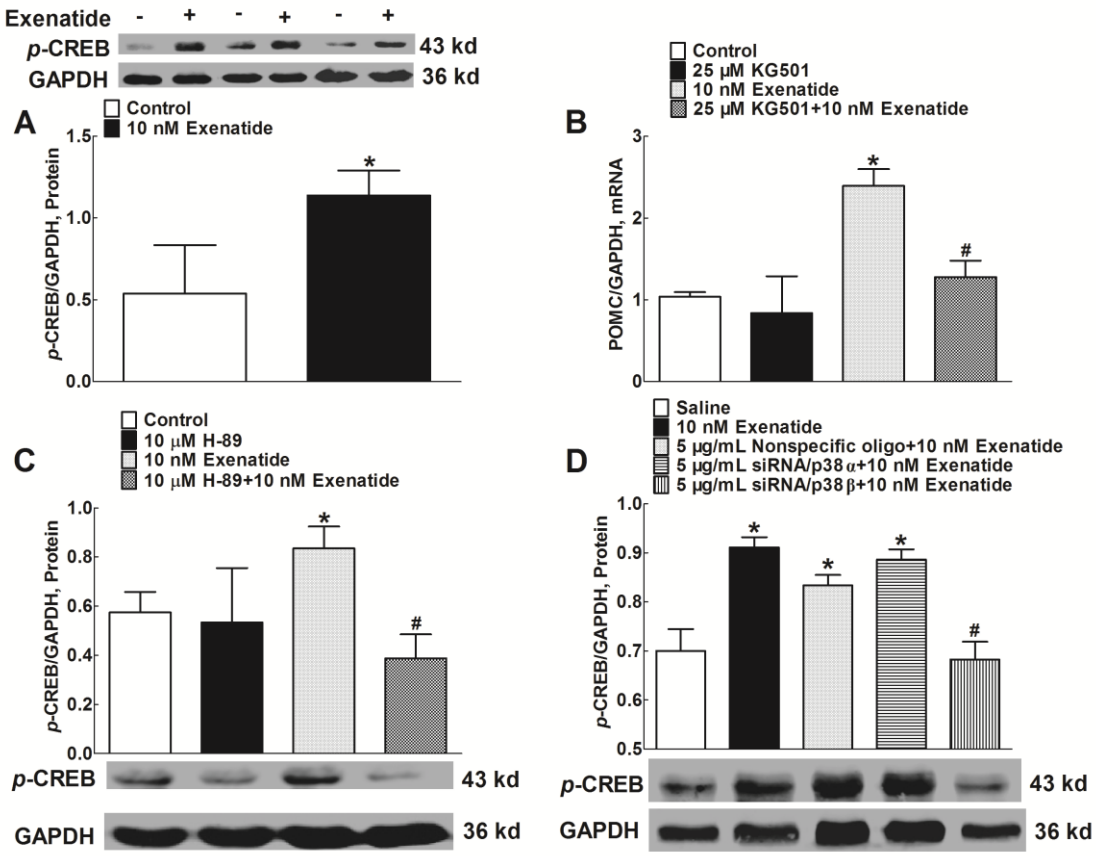

Molecular Pharmacology Fast Forward. Published on February 15, 2017 as DOI: 10.1124/mol.116.107102
This article has not been copyedited and formatted. The final version may differ from this version.

Figure 8